Journal of Hazardous Materials 393 (2020) 122380

Contents lists available at ScienceDirect

Journal of Hazardous Materials

journal homepage: www.elsevier.com/locate/jhazmat

Beyond graphene oxide acidity: Novel insights into graphene related materials effects on the sexual reproduction of seed plants

Fabio Candotto Carniel[a,*], Lorenzo Fortuna[a], Massimo Nepi[b], Giampiero Cai[b], Cecilia Del Casino[b], Giampiero Adami[c], Mattia Bramini[d,1], Susanna Bosi[c], Emmanuel Flahaut[e], Cristina Martín[f], Ester Vázquez[f,g], Maurizio Prato[c,h], Mauro Tretiach[a]

[a] Department of Life Sciences, University of Trieste, via L. Giorgieri 10, I-34127, Trieste, Italy
[b] Department of Life Sciences, University of Siena, via P. A. Mattioli 4, I-53100, Siena, Italy
[c] Department of Chemical and Pharmaceutical Science, University of Trieste, via L. Giorgieri 1, I-34127, Trieste, Italy
[d] Center for Synaptic Neuroscience, Italian Institute of Technology, Largo Rosanna Benzi 10, I-16132, Genova, Italy
[e] CIRIMAT, Université de Toulouse, CNRS, INPT, UPS, UMR CNRS-UPS-INP N° 5085, Université Toulouse 3 Paul Sabatier, Bât. CIRIMAT, 118, route de Narbonne, F-31062, Toulouse cedex 9, France
[f] Department of Organic Chemistry, Faculty of Chemical Science and Technology, University of Castilla-La Mancha, Av. Camilo José Cela, s/n, E-13005, Ciudad Real, Spain
[g] Instituto Regional de Investigación Científica Aplicada (IRICA), Universidad de Castilla-La Mancha, E-13071, Ciudad Real, Spain
[h] Carbon Nanobiotechnology Laboratory CIC BiomaGUNE, Paseo de Miramón 182, E-20009, Donostia-San Sebastian, Spain

GRAPHICAL ABSTRACT

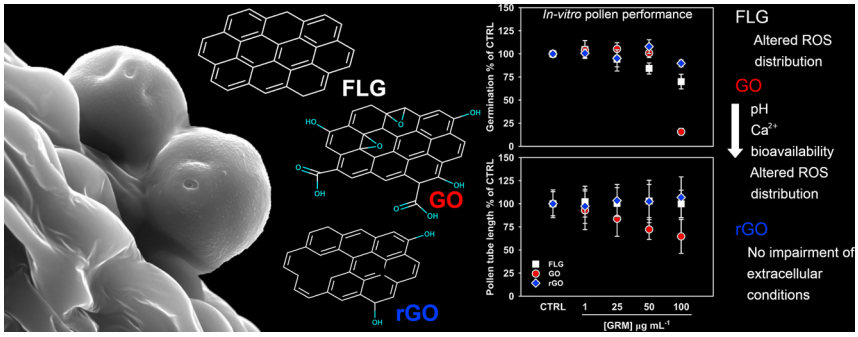

ARTICLE INFO

Editor: R. Debora

Keywords:
Calcium imbalance
Ecotoxicity
Graphene oxide
Nanomaterials
Phytonanotechnology

ABSTRACT

Graphene related materials (GRMs) are currently being used in products and devices of everyday life and this strongly increases the possibility of their ultimate release into the environment as waste items. GRMs have several effects on plants, and graphene oxide (GO) in particular, can affect pollen germination and tube growth due to its acidic properties. Despite the socio-economic importance of sexual reproduction in seed plants, the effect of GRMs on this process is still largely unknown. Here, *Corylus avellana* L. (common Hazel) pollen was germinated *in-vitro* with and without 1 − 100 µg mL^{-1} few-layer graphene (FLG), GO and reduced GO (rGO) to identify GRMs effects alternative to the acidification damage caused by GO. At 100 µg mL^{-1} both FLG and GO

* Corresponding author at: via L. Giorgieri 10, I-34127, Trieste, Italy.
E-mail addresses: fcandotto@units.it (F. Candotto Carniel), lfortuna@units.it (L. Fortuna), massimo.nepi@unisi.it (M. Nepi), giampiero.cai@unisi.it (G. Cai), cecilia.delcasino@unisi.it (C. Del Casino), gadami@units.it (G. Adami), Mattia.Bramini@iit.it (M. Bramini), sbosi@units.it (S. Bosi), flahaut@chimie.ups-tlse.fr (E. Flahaut), c.martin-jimenez@ibmc-cnrs.unistra.fr (C. Martín), Ester.Vazquez@uclm.es (E. Vázquez), prato@units.it (M. Prato), tretiach@units.it (M. Tretiach).
[1] Present address: Department of Applied Physics, Faculty of Science, University of Granada, C/Fuentenueva s/n, E-18071, Granada, Spain.

https://doi.org/10.1016/j.jhazmat.2020.122380
Received 20 December 2019; Received in revised form 14 February 2020; Accepted 21 February 2020
Available online 22 February 2020

Pollen

decreased pollen germination, however only GO negatively affected pollen tube growth. Furthermore, GO adsorbed about 10 % of the initial Ca^{2+} from germination media accounting for a further decrease in germination of 13 % at the pH created by GO. In addition, both FLG and GO altered the normal tip-focused reactive oxygen species (ROS) distribution along the pollen tube. The results provided here help to understand GRMs effect on the sexual reproduction of seed plants and to address future *in-vivo* studies.

1. Introduction

Graphene is a 2D carbon-nanomaterial of extraordinary chemical and physical properties with manifold applications ranging from electronics and energy storage to medicine (Novoselov et al., 2012). Considered the material of the future, new devices containing GRMs from bike- (https://www.vittoria.com/eu/tire-technology) and car tyres US Pat., No. 7999027, to asphalts for road paving (Zeng et al., 2017), printer powders, touch panels, smart windows or phones and medical devices are becoming more ubiquitous in society. Although the benefits gained by GRMs are without question, the increased production and rapid spread of GRM-containing products could have unpredictable drawbacks. It is reasonable to assume that these products will age, wear out and eventually be disposed of, causing an inevitable release of GRM particles into the environment (Fadeel et al., 2018). At the same time, GRMs could be released directly into the environment during production processes, as drug-enhancers and carriers (Wang et al., 2019a,b; Miraftab and Xiao, 2019), by applications imposing aerial dispersions on plants such as GRM-composites used to fight crop diseases (Chen et al., 2014; Liu et al., 2017; Wang et al., 2019a,b) or as carriers for plant fertilizers (An et al., 2017; Kabiri et al., 2017; Zhang et al., 2014). Considering the extreme lightweight nature of these materials, GRM nanoparticles could feasibly be dispersed into the air in the same way that fine and ultrafine particulate matter (PM) is. Once airborne, they may be transported for long distances, as reported for carbon black (Ramanathan and Carmichael, 2008; Qi and Wang, 2019), eventually landing onto vegetation, which is a natural trap of PM (Litschke and Kuttler, 2008; Wang et al., 2019a,b). This premise raises important concerns about the possible negative effects of GRMs on crops. At present, widely varying effects of GRMs on the vegetative body of seed plants have been reported, possibly owing to different experimental conditions (materials, concentrations, exposure time, *etc.*), plant developmental stages (seed, seedling, adult plants) and/or species tested (Anjum et al., 2013; Begum et al., 2011; Begum and Fugetsu, 2013; Wang et al., 2014). Generally, GO is deemed to exert greater toxicity with respect to pristine graphene, FLG or rGO (Gonzáles-Domínguez et al., 2018; Montagner et al., 2017) likely owing to the higher number of oxygen functional groups which increase both reactivity and dispersion in water (Dreyer et al., 2010). Recently, the effect of GO on pollen performance of two crop species, *Nicotiana tabacum* L. (Tobacco plant) and *Corylus avellana* L. (common Hazel) was tested in *in-vitro* experiments (Candotto Carniel et al., 2018). The authors highlighted GO acidity as the main factor affecting pollen performance. However, other properties of GO might have contributed to the effects observed. It is known that GO can adsorb cations from aqueous solutions according to the density of oxygen functional groups spread over the graphene lattice (Chowdhury et al., 2015). Specific cations such as Ca^{2+}, play a fundamental role in germination and elongation of the pollen tube (Holdaway-Clarke and Hepler, 2003), hence their removal could also affect pollen performance. Furthermore, GO can cause an overproduction of ROS as a result of its internalization (Seabra et al., 2014) or itself may act as a ROS promoter (Zhang et al., 2012). Other massively produced GRMs (such as FLG and rGO) may also affect pollen performance. These materials possess a higher C/O ratio than GO, and are therefore predictably less reactive, but still hard and sharp, *i.e.* they can cause mechanical damage, cutting through cells and tissues (Chiacchiaretta et al., 2018; Zhao et al., 2017). This evidence, along with previous findings on the negative effects of Ag- and Pd-nanoparticles - as well as heavy metals - on pollen performance and plant productivity (Speranza et al., 2010, 2013; Song et al., 2018) raise further concerns about GRMs safety on the sexual reproduction of seed plants. The success of this delicate process strongly relies on pollination mechanisms, as well as on the intimate interaction between pollen grains and the stigmatic surface of the ovary. Gaining more insight into the effects of GRMs on the plant reproduction process would enable us to predict future scenarios and perhaps to adopt measures to make safer-by-design GRMs and derived applications.

Here, we tested the following hypotheses: (*i*) GO might interfere with the sexual reproduction process of seed plants by an effect that is alternative to its acidic property and (*ii*) other GRMs might be potentially dangerous owing to their chemical or physical properties. Building upon previous work (Candotto Carniel et al., 2018), we were interested to identify diverse and potentially harmful effects of GRMs other than GO acidification on the pollen performance of *Corylus avellana* L., an economically and ecologically important seed plant.

2. Materials and methods

2.1. Preparation and characterization of GRMs

Few-layer graphene was produced from pure graphite as per Gonzáles-Domínguez et al. (2018) while GO was produced by oxidation of carbon fibres in sulfuric acid with sodium nitrate at 0 °C (GANF Helical-Ribbon Carbon Nanofibres, GANF®) and provided by Grupo Antolin (Burgos, S). Reduced GO was produced by direct reduction of GO in H_2 atmosphere at 1000 °C for 2 h; rGO can in this way be easily compared with GO because only the surface chemistry is anticipated to be modified by the reduction treatment. Dry GRMs were re-suspended in water and sonicated in an ultrasonic bath prior to the experiments (Gonzáles-Domínguez et al., 2018). Raman analysis of GRMs was carried out with an inVia Raman Microscope (Renishaw, UK). The dispersions were drop-cast onto a Si wafer and dried on a hot plate. At least 30 Raman measurements were collected for each material in different locations at 532 nm with a 100× objective and an incident power of 1 mW μm^{-2}. Quantitative elemental analysis of FLG and GO was performed with a LECO CHNS-932 elemental analyser (LECO Corporation, USA) for C, H, N and O. GRMs were also characterized with a JEM 2100 high-resolution transmission electron microscope (HRTEM) (JEOL Ltd, JP). Stable dispersions of the materials were drop-cast onto nickel grids (3 mm, 200 mesh), dried under vacuum, and observed at an accelerating voltage of 200 kV. Lateral dimension distribution of GRMs was calculated with Fiji software.

2.2. Acquisition and preparation of pollen material

Pollen of *C. avellana* was collected (January 2018) from 15 native trees in the Karst (Trieste, NE Italy) far from sources of pollution. Twigs bearing unripe catkins were sampled and immediately transported to the laboratory; their bases were cut under water and kept immersed until flowers ripening and stamen dehiscence (c. 48 h at 20 °C, under dim light). Harvested pollens were sieved through 100 and 60 µm mesh sizes to remove debris, then dehydrated over silica-gel (RH ~ 5%) for 48 h and stored at -20 °C.

2.3. Germination of C. avellana pollen

Aliquots of thawed pollen of *C. avellana* were rehydrated in a closed chamber at c. 100 % RH for 3 h prior to use. Pollen germination was induced according to Candotto Carniel et al. (2018) in Brewbaker and Kwack's (BK) medium (Brewbaker and Kwack, 1963) containing 1.62 mM H_3BO_3, 1.25 mM $CaCl_2{\cdot}2H_2O$, 2.97 mM KCl and 1.65 mM $MgSO_4{\cdot}7H_2O$, with a pH of 6.3. To assess the effects of FLG, GO and rGO, pollen was germinated in BK medium without GRMs (control samples) and with GRM suspensions to a final concentration of 1, 25, 50 or 100 μg mL^{-1} (treated samples). Germination experiments were performed at 25 °C under dim light. Control and treated samples were gently shaken with a tilting agitator throughout the experiment in order to avoid sedimentation of GRMs. Three to four replicates were prepared for both control and treated samples. A parallel set (n = 3) of control and BK medium enriched with 100 μg mL^{-1} GRMs, with or without sucrose was prepared to assess the cation (Ca^{2+}, K^+, Mg^{2+}) adsorption capacity of GRMs during the pollen incubation period (3 h).

2.4. Assessment of pollen performance and viability

Pollen performance, *i.e.* germination percentage and pollen tube length, of control and treated samples was measured after 3 and 5.5 h. Images of germinating pollen were taken using a Zeiss Axiocam MRm camera connected to a Zeiss Axiophot microscope (Zeiss, D). Percentage germination was calculated by scoring at least 150 randomly selected grains. Grains were considered to have germinated if the pollen tube was longer than the average diameter of the pollen grains. Pollen tube length was measured for at least 50 randomly selected pollen tubes.

The viability of *C. avellana* pollen grains was evaluated in control and treated samples (100 μg mL^{-1} FLG and GO only) with the fluorescein diacetate (FDA) based fluorochromatic reaction test (Heslop-Harrison et al., 1984). Evaluation of percentage viability was done on at least 150 pollen grains for each sample.

2.5. Transmission electron microscopy (TEM)

TEM observations were made on controls and treated samples, with FLG and GO suspensions at 50 μg mL^{-1} and with 100 μg mL^{-1} GO suspension basified to pH 6.5 (*i.e.* the same as the control samples) to exclude effects induced by the acidic environment. Samples were fixed with a solution of 2% paraformaldehyde and 1.6 % glutaraldehyde in phosphate buffer at pH 6.9 for 45 min at room temperature. The pollens were then rinsed in the same buffer and post-fixed in 2% OsO_4 and 0.1 M sodium cacodylate buffer pH 7.4 for 2 h. Thereafter, they were washed 3 × 15 min in phosphate buffer and then dehydrated in a graded series of ethanol (30, 50, 70, 80, 90, 96 and 100 %) for at least 20 − 30 min for each concentration. Samples were embedded in epoxy resin according to the manufacturer's instructions. Using a Top 150 ultra-microtome (Pabisch, D), 110 nm thin sections were collected onto copper mesh grids and observed with a Philips EM208 electron microscope operating at 100 kV and equipped with a Quemesa EMSIS camera (EMSIS, D).

2.6. FLG, GO and rGO cation adsorption capacity

To assess the capacity of GRMs to adsorb the dissolved cations (Ca^{2+}, K^+ and Mg^{2+}) in BK medium during the pollen incubation period, 1 mL of the control (n = 3) and 100 μg mL^{-1} GRMs-enriched suspensions n = 3 with and without sucrose but free from pollen (see 2.3) were centrifuged at 17,000 × g for 15 min to pellet the GRMs. 800 μL of supernatant was then recovered and added to 8 μL of HNO_3 (69.5 % v/v), heated for 1 h, diluted with Milli-Q water to 10 mL and filtered through a GHP Acrodisc syringe filter (pore size 0.45 μm). Analysis was carried out with an Optima 8000 ICP-OES (Perkin Elmer, USA). A calibration curve was obtained by diluting a standard solution (Sigma-Aldrich, USA) in the range 0–10 mg L^{-1}. The precision of the measurements as relative standard deviation were always < 5%. LOD at 317.9 (Ca^{2+}), 285.2 (Mg^{2+}) and 766.5(K^+) nm were 0.02, 0.01 and 0.01 mg L^{-1}, respectively.

2.7. Evaluation of the synergistic effect of Ca^{2+} and pH decrease on pollen performance

The effect of decreased Ca^{2+} in BK medium on pollen performance due to the presence of GRMs was evaluated by germinating pollen in standard BK medium (control samples) and in BK medium prepared with Ca^{2+} concentration decreased by -10, -20 and -30 % (treated samples) with respect to the control. In addition, the same experiment was repeated with BK medium acidified to pH 4.2, *i.e.* the pH of a 100 μg mL^{-1} GO suspension in BK medium (Candotto Carniel et al., 2018).

2.8. Analysis of ROS distribution in growing pollen tubes

Reactive oxygen species in pollen tubes were detected using dichlorofluorescin diacetate ($DCFH_2$-DA) dye dissolved in DMSO (Molecular probes, USA) according to Pasqualini et al., (2011). A concentrated solution (25 mM) of dye was diluted in BK medium to 5 μM. 15 μL of control and treated (100 μg mL^{-1} FLG or GO only) pollen culture was poured onto a glass slide after 3 and 5.5 h of germination;15 μL of the diluted $DCFH_2$-DA was added to achieve a final concentration of 2.5 μM. Observations were made after the mixture had been left to react in the dark room for one minute or so. Negative controls (without the dye) were also prepared to detect and remove any background noise. Images were taken in the microscopy facility mentioned above and analysed using ImageJ software (Wayne Rasband, NIH, USA).

2.9. Data analysis

Measurements of pollen performance and fluorescence signal from FDA and $DCFH_2$-DA respectively were made using ImageJ software (version 1.51J8) after calibration of images with the scale bar command of the Axiovision software (Zeiss, D).

The effect of GRMs on pollen performance was assessed using a factorial experimental design which considered GRMs (FLG, GO and rGO), their concentrations (0, 25, 50 and 100 μg mL^{-1}) and pollen incubation time (3 and 5.5 h) as categorical factors. Values of pollen germination percentage and pollen tube length from control and treated samples were statistically compared with a factorial ANOVA followed by Tuckey's HSD post-hoc test. The same statistical analysis was carried out for results of the Ca^{2+}/pH experiment (Section 2.7), whose experimental design considered Ca^{2+} concentration (1.250, 1.125, 1.000 and 0.875 mM), pH of BK medium (6.3 and 4.2) and germination times as categorical factors. In order to exclude bias due to slow growing pollen tubes (or to pollens which stopped growing) only the values of the 30 % longest tubes were selected for analysis. The length of pollen tubes measured in each replicate was first expressed as a percentage with respect to the mean tube length measured in control samples and then averaged in accordance with each experimental condition. Pollen viability data based on the fluorescence signal from FDA were analyzed by Two-Way ANOVA followed by Fisher's LSD post-hoc test using GRMs type and incubation time as categorical factors. All calculations were carried out with Microsoft Office Excel 2010 (Microsoft corporation, USA) and STATISTICA 6.0 (StatSoft Inc., USA).

3. Results and discussion

3.1. GRMs characterization

The GRMs (FLG, GO and rGO) tested in this work were chosen

because of differences deriving from the presence or absence of defects and oxygen functional groups in the graphene lattice, and because of their lateral dimensions. These features are mostly exploited to develop new composite materials and technological applications but they are also at the root of various effects that GRMs may exert on organisms. The physical and chemical analyses highlighted these differences. The Raman spectrum of FLG has the two most intense peaks of graphene appearing at ~1580 and ~2700 cm^{-1}, the G and the 2 D bands respectively (Fig. S1 A). The I(2D)/I(G) ratio is 0.44 on average, consistent with the value (< 1) usually assigned to FLG (Ferrari et al., 2006; Mogera et al., 2015). The appearance of a further band with peak at ~1345 cm^{-1} (D band) (Fig. S1 A) suggests the presence of defects on the graphene lattice. In this case, the average spectrum of FLG has an I(D)/I(G) of 0.34 suggesting a low level of defects. On the contrary, the Raman spectrum of GO had broad D and G bands (Fig. S1 a), the absence of a clear 2D band and an I(D)/I(G) of 1.03 revealing a rather disordered material. Similarly, the Raman spectrum of rGO had broad D and G bands but an higher I(D)/I(G) (1.50) indicating the presence of defects that were likely to be caused by the reduction process which removed the oxygen functional groups, leaving holes and irregularities in the graphene lattice. These GRMs differed in elemental composition; FLG and rGO were comprised of > 95 % C, compared to GO which was comprised of > 40 % O atoms (Fig. S1 b) confirming a high presence of oxygen functional groups in the graphene lattice. TEM image analysis showed that FLG flakes had the most homogeneous distribution of lateral dimensions ranging from 100-750 nm. Similarly, > 90 % of GO and rGO flakes were of similar sizes to FLG, but aggregates with larger dimensions were also detected (Fig. S1 c–f).

3.2. In-vitro performance and viability of pollen exposed to GRMs

The pollen grain is the plant microgametophyte, a minuscule vehicle which has the paramount role of delivering the male nuclei undamaged to the egg-cell. Any harmful effect on pollen could therefore result in limiting the success of the fertilization process, resulting in decreased seed production. After 5.5 h of incubation, germination percentage of control pollen was always > 60 % with an average pollen tube length > 80 µm. Exposure to FLG and GO (but not rGO) significantly affected pollen performance with differing effects according to the type and concentration of materials (see Tab. S1). With addition of FLG, pollen germination remained steady up to 25 µg mL^{-1}, but then progressively decreased by 30 % and 32 % after 3 h and 5.5 h of FLG exposure respectively, at 100 µg mL^{-1} (Figs. 1a and S2a). Pollen germination was not affected by exposure to GO up to 50 µg mL^{-1}, but decreased by 84 % and 83 % after 3 and 5.5 h of GO exposure respectively, at 100 µg mL^{-1} (Figs. 1a and S2a). Pollen tube elongation was affected only by GO, progressively decreasing with the increased concentration, reaching 32 % and 50 % of the control value at 100 µg mL^{-1} after 3 and 5.5 h exposure to GO, respectively (Figs. 1b and S2b). Despite the important effects observed above when pollen was exposed to the highest concentrations of FLG and GO, the viability of pollen was never significantly affected and maintained values ≥ 86 % in comparison with control samples (Table S3). Candotto Carniel et al. (2018) showed that GO affects pollen performance predominately due to its acidic properties deriving from oxygen functional groups spread over the graphene lattice (Dimiev et al., 2013). However, FLG is not acidic as it lacks the above-mentioned groups (Fig. S1). Hence, we anticipate that the interaction mechanisms involved in pollen performance decrease caused by FLG and GO are different. GRMs may adversely affect pollen performance by other means such as direct contact with cells, *i.e.* the sharp and hard edges of GRMs can act as nano-blades cutting through the plasma membrane (Tu et al., 2013) and also through the thin cell-wall of some freshwater algae (Zhao et al., 2017). In addition GRMs flakes that become internalized can disrupt cell cytoskeleton (Chiacchiaretta et al., 2018) and affect the normal intracellular redox state by impairing the membrane potential of mitochondria (Pelin et al., 2018; Zhang et al., 2012) thus causing an oxidative burst and/or act directly as ROS promoters in the presence of other ROS normally produced by the aerobic metabolism, such as H_2O_2. Reduced GO had no effect on pollen performance (Zhang et al., 2012). The presence of big, non-dispersible aggregates in the rGO suspension (Fig. S1c) might have decreased the real number of small flakes deemed to cause mechanical and oxidative damage (Liu et al., 2014). In addition, the rGO used here had a C/O ratio comparable to that of FLG (see Fig. S1) *i.e.* it was almost inert, a feature that helps to explain the absence of negative effects on pollen performance. In fact, rGO estimated as toxic to bacteria (Guo et al., 2017) and fresh freshwater algae (Zhao et al., 2017) had an oxygen content ≥ 20 %.

3.3. Effects of FLG and GO on pollen grain and pollen tube ultrastructure

The pollen grain is protected by a thick and sturdy barrier (the pollen wall) which confers resistance to a variety of adverse factors such as mechanical damage, UV light, high temperatures, microbial attack and water loss (Jiang et al., 2013). In this study we attempted to verify with TEM whether FLG and GO flakes damaged or obstructed apertures (in this case three *colpori*) of the pollen grains from which the pollen tubes germinate and/or if they affected the soft, elastic pollen tube in the first stages of germination. At 50 (FLG and GO) and 100 µg mL^{-1} (GO), GRM caused no ultrastructural modification to the germinating pollen at the pore level (Fig. 2). FLG was not observed to accumulate around the pores (Fig. 2b) and was rarely detected adhering to pollen grains (Fig. 2d) which may be explained by the lower potential of FLG (than GO) to bind to the surrounding environment. We also considered if the sample preparation for the TEM analysis might have removed the majority of FLG flakes from the pollen as has

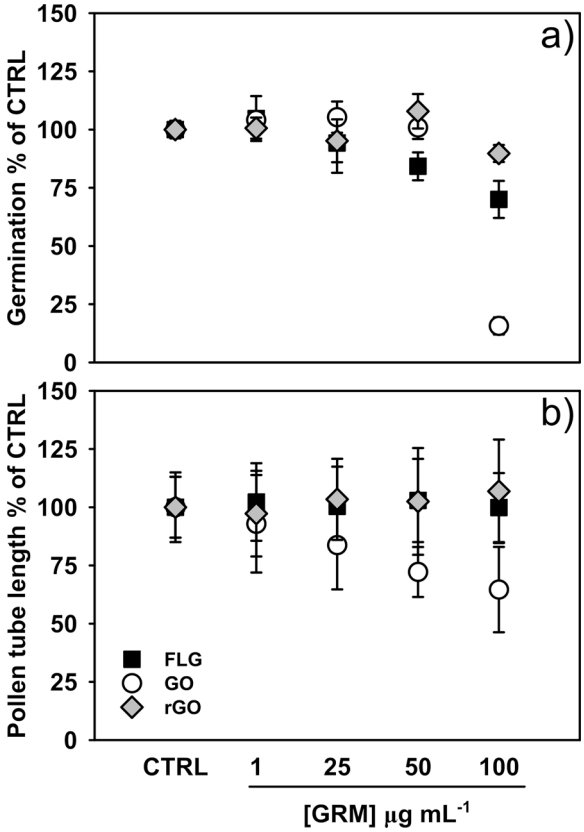

Fig. 1. GRMs effect on *C. avellana* pollen performance. Germination percentage (a) and tube length (b) after 3 h of incubation in BK without (CTRL) and with 1, 25, 50 and 100 µg mL^{-1} of FLG, GO or rGO. Values are reported as means ± 1 st. dev. (n = 450 for a; n ≥ 50 for b). Statistically different groups are reported in Table S1.

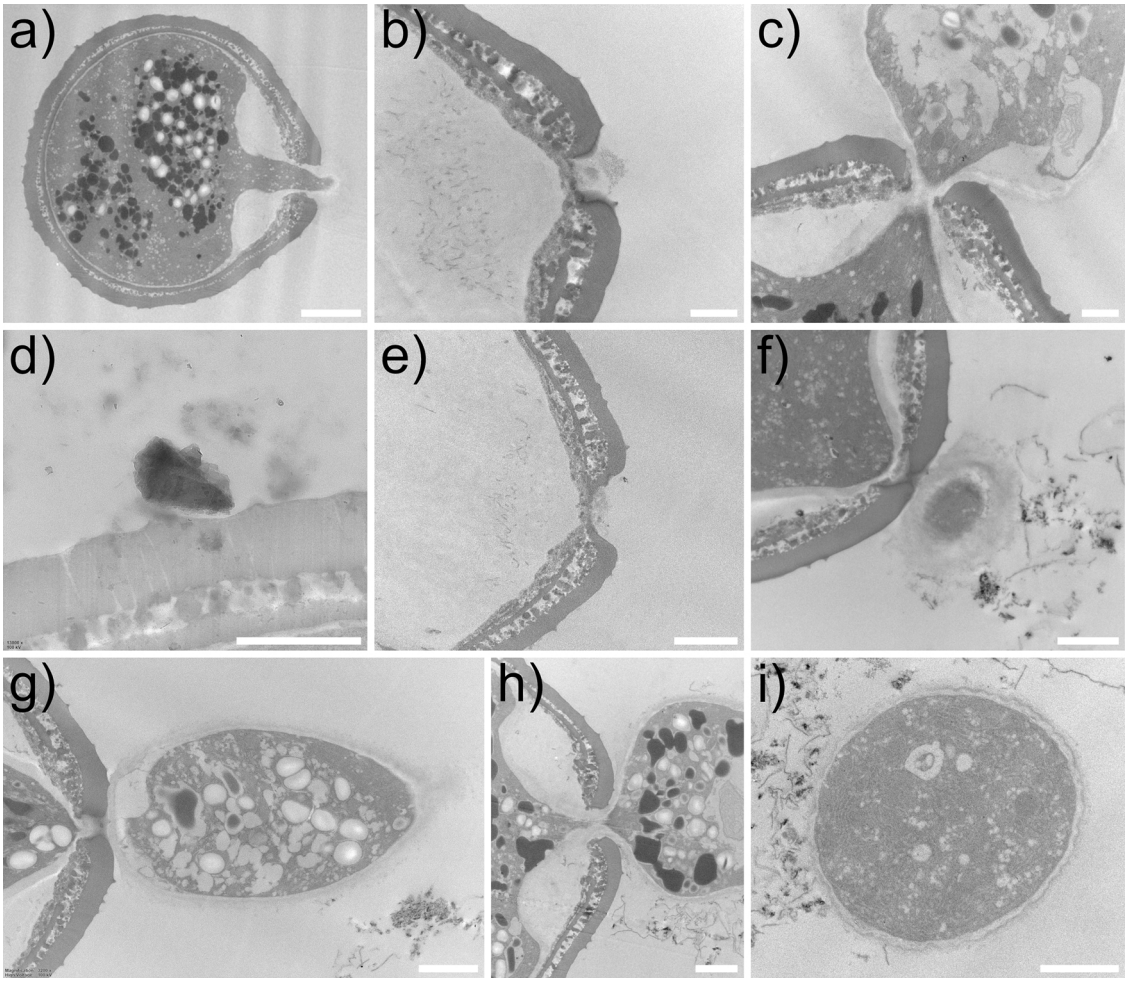

Fig. 2. Micrographs of germinating *C. avellana* pollen observed by TEM. Pollen grains were incubated in BK medium without (a) and with FLG (b–d) and GO (e–i) at 50 μg mL^{-1} (b–f) and in BK with GO at 100 μg mL^{-1} and pH of 6.3 (g-i) 3 h. Scale bars = 4 μm (a); 1 μm in (b–d); 2 μm (e–i).

previously been observed by Banchi et al. (2019). Conversely, GO was frequently observed around the pectinic layer surrounding the base of the germinating pollen tube (Fig. 2f) or the pollen tube itself (Fig. 2g–i) confirming previous observations on *N. tabacum* L. and *C. avellana* L. pollen treated at the same GO concentration (Candotto Carniel et al., 2018). In any case, GRMs flakes cutting through the pollen wall or the cell wall of pollen tubes [as observed in *Chlorella pyrenoidosa* (Zhao et al., 2017)] was never observed; nor was GRMs internalization in the pollen grains or tubes detected. These results confirm that the cell wall of pollen grains and tubes respectively, are biological barriers that can hardly be harmed by GRM flakes.

3.4. GRMs cation adsorption capacity and related in-vitro effects on pollen performance

Graphene oxide possesses different oxygen functional groups spread over the graphene lattice such as carboxyls which confer acidity, and carbonyls and epoxides that can bind cations dissolved in aqueous solution in the surrounding environment (Chowdhury et al., 2015). Adsorption of cations by GO may be a limiting factor to pollen germination and growth as Ca^{2+} plays a critical role in this process (Holdaway-Clarke and Hepler, 2003). In fact, Ca^{2+} has many important effects: Ca^{2+} currents have been detected at germination sites suggesting an active role in pollen germination; also, release of Ca^{2+} from endoplasmic reticulum is critical to pollen tube growth as well as growth polarity (Holdaway-Clarke and Hepler, 2003). As such, calcium ions can be involved in at least two processes: modulation of the organisation of actin filaments (Aloisi et al., 2017) and cell-wall strengthening. Extracellular Ca^{2+} is also involved in the extension of the cell-wall at the pollen tube tip by binding adjacent acidic pectins thus making the cell wall more rigid (Domozych et al., 2013). In this study 100 μg mL^{-1} GO significantly decreased the content of Ca^{2+} and Mg^{2+} (but not K^{+}) within BK medium (9.0 and 5.3 %, respectively) compared to FLG and rGO which did not (Fig. 3). This effect was reduced in BK medium without sucrose (see Fig. S3) suggesting that Ca^{2+} and Mg^{2+} may create bonds between GO and other organic molecules as observed by Jiang et al. (2017). Moreover, a decrease in Ca^{2+} oscillations and intracellular storage has already been seen in primary astrocytes upon GO exposure, while FLG did not alter the normal Ca^{2+} homeostasis (Bramini et al., 2019). The effect of decreased Ca^{2+} in the presence of 100 μg mL^{-1} of GO was simulated *in-vitro* on the pollen performance of *C. avellana* either at sub-neutral (pH 6.3) and acidic (pH 4.2) conditions. Both conditions significantly affected pollen performance (Table S4). In the first case, pollen germination was significantly affected when Ca^{2+} was reduced by 30 % with respect to normal BK medium (Fig. 4a), whereas pollen tube growth was significantly affected when Ca^{2+} was reduced by 20 % (Fig. 4b). According to Candotto Carniel et al. (2018), both pollen germination and tube growth were significantly affected under acidic conditions with respect to control BK medium (38 % and 44 %, respectively; Fig. 4a). Interestingly, pollen germination further decreased by another 13 % when Ca^{2+} was decreased by 10 % (Fig. 4a). These results highlight that GO may interfere with sexual reproduction of seed plants not only owing to its acidity but also due to its capacity to immobilize or adsorb cations

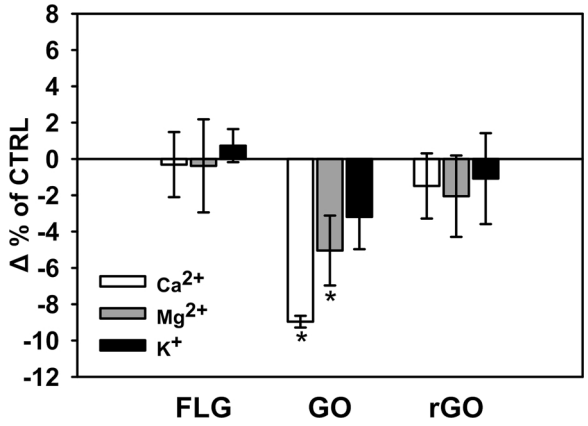

Fig. 3. GRMs adsorption capacity towards cations. Variation (Δ) of Ca^{2+}, Mg^{2+} and K^{+} in BK medium after 3 h with 100 μg mL^{-1} of FLG, GO and rGO. Values are reported as means ± 1 st. dev. (n = 3). Groups statistically different from CTRL are marked with * (One-way Anova, Fisher's LSD test).

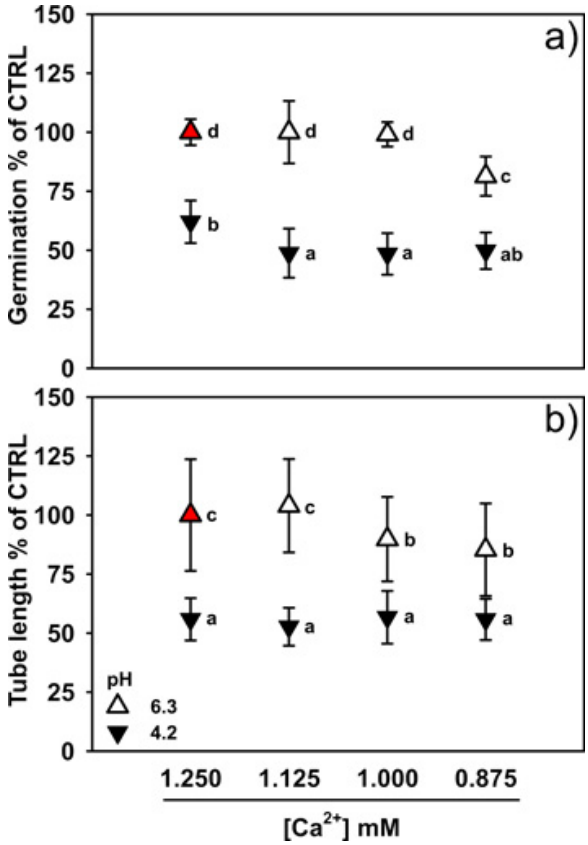

Fig. 4. Effect of Ca^{2+} and/or pH decrease on *C. avellana* pollen performance. Pollen germination percentage (a) and tube length (b) after 3 h of incubation in BK (CTRL: red triangle), BK with a decreased Ca^{2+} concentration, pH or both. Values are reported as means ± 1 st. dev. [n = 450 for a); n ≥ 50 for b)]. Statistically different groups are marked with different letters (Two-way Anova, Fisher's LSD test) (For interpretation of the references to colour in this figure legend, the reader is referred to the web version of this article).

from the environment. In light of the important role of Ca^{2+}, an imbalance of extracellular bioavailability of this cation due to the presence of GO could result in decreased pollen germination caused by reduced pH (see Fig. 4a). It is likely that an excess of protons in the extracellular media could interfere with calcium ions binding to acidic pectins, thereby causing alterations in growth processes.

3.5. ROS distribution along the pollen tube in GRMs-treated pollen

The signalling system involved in pollen tube growth involves tip-focused ROS production triggered by Ca^{2+} *via* NADPH oxidases (Cardenas et al., 2006; Potocký et al., 2007; Suzuki et al., 2011). ROS imbalance at the cellular level is one of the most commonly reported negative effects of GRMs (Montagner et al., 2017). On the basis of Ca^{2+} adsorption results, we were interested to see whether ROS distribution along the pollen tube was affected by those GRMs that had an effect on pollen performance. In control samples, ROS were distributed according to the common tip-focused gradient (Fig. 5a), *i.e.* the presence of ROS increased from the base to the pollen tip where pollen tube growth takes place (Domozych et al., 2013). In samples treated with 100 μg mL^{-1} FLG or GO, two distinct ROS distribution patterns that differed from controls were recognized. In FLG treated pollens, ROS were distributed irregularly along the pollen tube with spots of great intensity (Fig. 5c, d). In GO treated pollens, ROS were homogeneously distributed along the pollen tube (Fig. 5e, d). In both cases, impaired ROS distribution may result in impaired pollen tube growth. In the case of FLG, evidence suggesting a possible interaction mechanism (such as internalization or pollen tube damage) was not found. However, taking into account previous observations of aero-terrestrial green micro alga *Trebouxia gelatinosa* (Banchi et al., 2019) we hypothesize that extremely small GRM flakes may have reached the cell-wall/cell membrane interface and interacted with membrane receptors causing localized ROS production. A similar mechanism could potentially be the cause of decreased germination observed at the highest FLG concentration used (100 μg mL^{-1}; Fig. 1a). Changed intracellular ROS distribution as a result of interaction of GO with the pollen tube may be related to the reactivity of this material. As shown with TEM, GO tends to adhere to the pollen tube cell-wall forming condensed patches of GO flakes. Owing to the capacity of GO to bind cation (especially Ca^{2+}) patches of flakes likely hindered the formation of the Ca^{2+} gradients occurring between the intra- and the extra-cellular space, especially at the tube tip level. As reported by Potocký et al. (2007) the local absence of Ca^{2+} fluxes does not allow NADPH oxidase activation which is responsible for accumulation of ROS at the pollen tube tip.

3.6. Relevance of the observed GRMs effects on in-vivo pollen performance

Negative effects on pollen performance induced by GO shown in this and in previous work (Candotto Carniel et al., 2018) could be relevant from a biological point of view, however the GRM concentration that causes an appreciable effect *in vitro*, *i.e.* 100 μg mL^{-1}, is unlikely to occur in the environment. The pH decrease caused by GO (probably the most important effect described so far) which negatively affects pollen performance *in-vitro*, might work quite differently *in vivo*, particularly at the stigmatic level. In fact, while studying the effects of acid rains, numerous authors have hypothesized that the stigmatic surface may have an intrinsic buffering capacity, which could explain discrepancies between *in vitro* and *in vivo* observations (Cox, 1984; Du Bay and Murdy, 1983; DuBay and Murdy, 1983; Wolters and Martens, 1987). Direct evidence of this buffering capacity is still not forthcoming, notwithstanding its evident importance. In this work, further negative effects of GO were described, *i.e.* decreased bioavailability of Ca^{2+} ions and impairment of ROS distribution along the pollen tube; both mechanisms play an important role in pollen tube growth (Holdaway-Clarke and Hepler, 2003). Thereafter, deposition of GO (even at low levels) could cause a localized imbalance of Ca^{2+} bioavailability, thus affecting ROS distribution of the growing pollen tubes, especially if the stigmatic surface suffers from acidification processes. At this stage it is difficult to predict whether the presence of GO might modify Ca^{2+} concentrations in stigmatic fluids, because the actual concentrations of this ion are largely unknown, despite the good knowledge about the localization and dynamics of Ca^{2+} along the pistil before and during flower anthesis (Ge et al., 2009; Zienkiewicz et al., 2011). Something

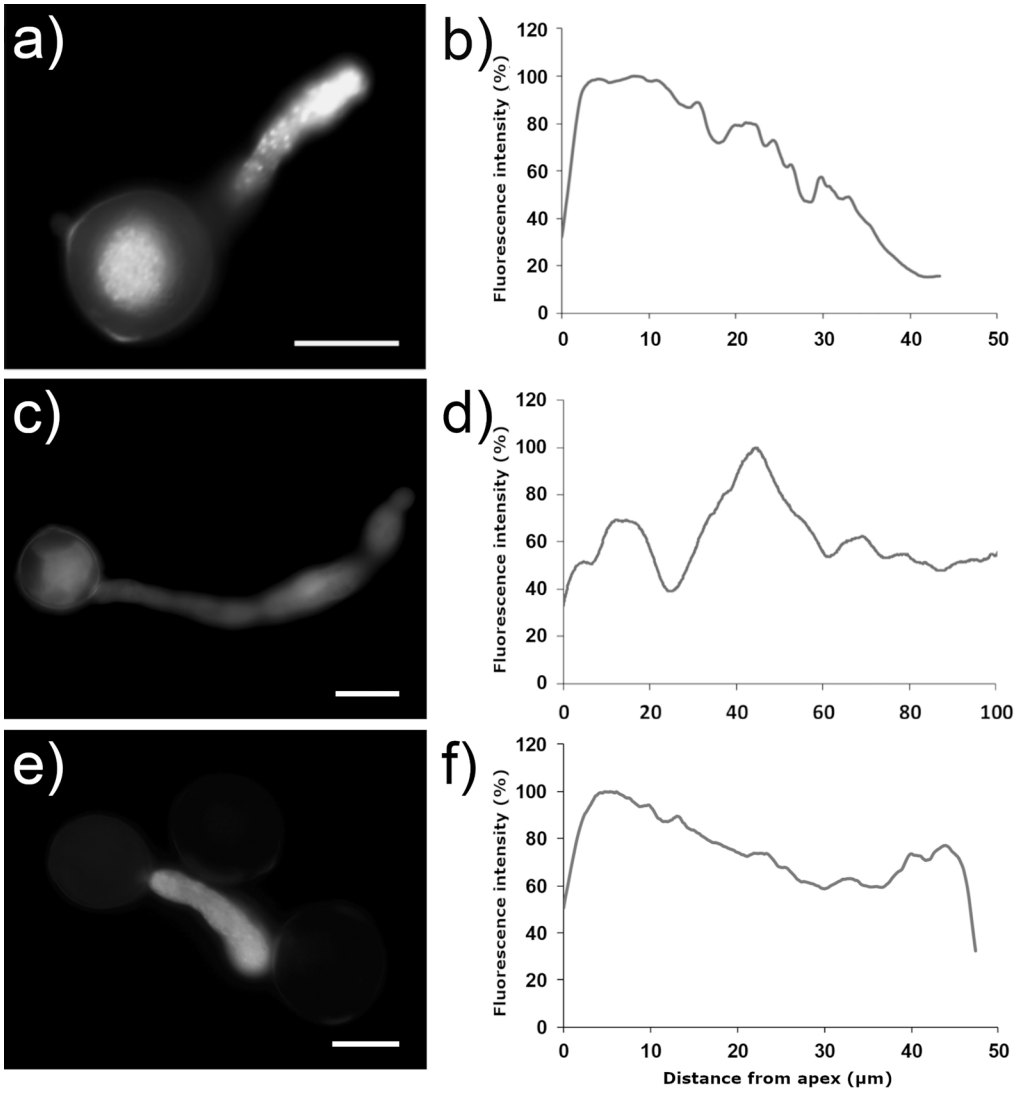

Fig. 5. ROS distribution along the pollen tube. DCFH2-DA fluorescence in pollen tubes incubated in BK medium without (a) and with 100 µg mL^{-1} of FLG (c) and GO (e) for 3 h. The corresponding $DCFH_2$-DA fluorescence intensities along the pollen tube are reported on the right panels (b, d, f). Scale bars = 20 µm.

similar may also occur with deposition of FLG, whose negative effects are also described here from an *in-vitro* perspective. Conversely, rGO appeared to be the safest GRM with respect to pollen performance of *C. avellana* suggesting that the full reduction of GO may be a valid method to decrease the ecotoxicological impact of GO-containing waste.

4. Conclusions

Using manipulative *in-vitro* experimentation, we showed that FLG and GO (but not rGO) may have an effect on pollen germination (FLG) and pollen tube growth (GO) of an economically and ecologically important seed plant, the common hazel. Decreased pollen germination in the presence of high FLG levels needs further clarification, but may be related to intracellular impairment of localized ROS production or to interactions of GRMs flakes with the intine layer at the pollen germination pore. Conversely, GO seems to affect pollen germination and tube growth by decreasing Ca^{2+} bioavailability, and (as a consequence) extinguishing the tip-focused ROS gradient along the pollen tube, thus interfering with both elongation and polarity. Furthermore, it was shown that the effect of decreased Ca^{2+} bioavailability is increased under acidic conditions, and this is especially important to pollen germination. These phenomena depend on indirect effects of GO in the media, *i.e.* by adsorption of cations and acidification (Candotto Carniel et al., 2018). In the light of the new results, the possible interference of FLG and GO on pollen germination needs further investigation at the stigmatic level.

CRediT authorship contribution statement

Fabio Candotto Carniel: Conceptualization, Methodology, Investigation, Writing - original draft, Visualization. **Lorenzo Fortuna:** Conceptualization, Methodology, Formal analysis, Writing - original draft. **Massimo Nepi:** Methodology, Writing - review & editing. **Giampiero Cai:** Methodology, Writing - review & editing. **Cecilia Del Casino:** Investigation. **Giampiero Adami:** Resources. **Mattia Bramini:** Investigation, Resources. **Susanna Bosi:** Investigation, Project administration. **Emmanuel Flahaut:** Resources, Writing - review & editing. **Cristina Martín:** Investigation, Writing - review & editing. **Ester Vázquez:** Resources, Writing - review & editing. **Maurizio Prato:** Funding acquisition, Resources, Project administration, Supervision, Writing - review & editing. **Mauro Tretiach:** Conceptualization, Visualization, Funding acquisition, Resources, Supervision, Writing - review & editing, Project administration.

Declaration of Competing Interest

The authors declare that they have no known competing financial interests or personal relationships that could have appeared to influence the work reported in this paper.

Acknowledgements

The authors like to thank Demi Vattovaz and Luigi Camerlenghi (Trieste), Marcella Lo Vullo and Silvia Licata (Siena), for the help provided in the lab, Prof. Piero Giulianini (Trieste) for the help and Dr. Marina Tretiach (Sydney, AUS) for English revision.

Funding

This work has received funding from the European Union's Horizon 2020 research and innovation programme Graphene Flagship under grant agreement No 785219 and by the Spanish Ministerio de Economía y Competitividad (project CTQ2017-88158-R).

Appendix A. Supplementary data

Supplementary material related to this article can be found, in the online version, at doi:https://doi.org/10.1016/j.jhazmat.2020.122380.

References

Aloisi, I., Cai, G., Faleri, C., Navazio, L., Serafini-Fracassini, D., Del Duca, S., 2017. Spermine regulates pollen tube growth by modulating Ca^{2+}-dependent actin organization and cell wall structure. Front. Plant Sci. 8. https://doi.org/10.3389/fpls.2017.01701.

An, D., Liu, B., Yang, L., Wang, T.J., Kan, C., 2017. Fabrication of graphene oxide/polymer latex composite film coated on KNO_3 fertilizer to extend its release duration. Chem. Eng. J. 311, 318–325. https://doi.org/10.1016/j.cej.2016.11.109.

Anjum, N.A., Singh, N., Singh, M.K., Shah, Z.A., Duarte, A.C., Pereira, E., Ahmad, I., 2013. Single-bilayer graphene oxide sheet tolerance and glutathione redox system significance assessment in faba bean (*Vicia faba* L.). J. Nanopart. Res. 15. https://doi.org/10.1007/s11051-013-1770-7.

Banchi, E., Candotto Carniel, F., Montagner, A., Bosi, S., Bramini, M., Crosera, M., León, V., Martín, C., Pallavicini, A., Vázquez, E., Prato, M., Tretiach, M., 2019. Graphene-based materials do not impair physiology, gene expression and growth dynamics of the aeroterrestrial microalga *Trebouxia gelatinosa*. Nanotoxicology 13, 492–509. https://doi.org/10.1080/17435390.2019.1570371.

Begum, P., Fugetsu, B., 2013. Induction of cell death by graphene in *Arabidopsis thaliana* (Columbia ecotype) T87 cell suspensions. J. Hazard. Mater. 1032–1041. https://doi.org/10.1016/j.jhazmat.2013.06.063.

Begum, P., Ikhtiari, R., Fugetsu, B., 2011. Graphene phytotoxicity in the seedling stage of cabbage, tomato, red spinach, and lettuce. Carbon 49, 3907–3919. https://doi.org/10.1016/j.carbon.2011.05.029.

Bramini, M., Chiacchiaretta, M., Armirotti, A., Rocchi, A., Kale, D.D., Martin, C., Vázquez, E., Bandiera, T., Ferroni, S., Cesca, F., Benfenati, F., 2019. An increase in membrane cholesterol by graphene oxide disrupts calcium homeostasis in primary sstrocytes. Small 15, 1900147. https://doi.org/10.1002/smll.201900147.

Brewbaker, J.L., Kwack, B.H., 1963. The essential role of calcium ion in pollen germination and pollen tube growth. Am. J. Bot. 50, 859–865. https://doi.org/10.1002/j.1537-2197.1963.tb06564.x.

Candotto Carniel, F., Gorelli, D., Flahaut, E., Fortuna, L., Del Casino, C., Cai, G., Nepi, M., Prato, M., Tretiach, M., 2018. Graphene oxide impairs the pollen performance of *Nicotiana tabacum* and *Corylus avellana* suggesting potential negative effects on the sexual reproduction of seed plants. Environ. Sci. Nano 5, 1608–1617. https://doi.org/10.1039/c8en00052b.

Cardenas, L., McKenna, S.T., Kunkel, J.G., Hepler, P.K., 2006. NAD(P)H oscillates in pollen tubes and is correlated with tip growth. Plant Physiol. 142, 1460–1468. https://doi.org/10.1104/pp.106.087882.

Chen, J., Peng, H., Wang, X., Shao, F., Yuan, Z., Han, H., 2014. Graphene oxide exhibits broad-spectrum antimicrobial activity against bacterial phytopathogens and fungal conidia by intertwining and membrane perturbation. Nanoscale 6, 1879–1889. https://doi.org/10.1039/c3nr04941h.

Chiacchiaretta, M., Bramini, M., Rocchi, A., Armirotti, A., Giordano, E., Vázquez, E., Bandiera, T., Ferroni, S., Cesca, F., Benfenati, F., 2018. Graphene oxide upregulates the homeostatic gunctions of primary astrocytes and modulates astrocyte-to-neuron communication. Nano Lett. 18, 5827–5838. https://doi.org/10.1021/acs.nanolett.8b02487.

Chowdhury, I., Mansukhani, N.D., Guiney, L.M., Hersam, M.C., Bouchard, D., 2015. Aggregation and stability of reduced graphene oxide: complex roles of divalent cations, pH, and natural organic matter. Environ. Sci. Technol. 49, 10886–10893. https://doi.org/10.1021/acs.est.5b01866.

Cox, R.M., 1984. Sensitivity of forest plant reproduction to long range transported air pollutants: *in vitro* and *in vivo* sensitivity of *Oenothera parviflora* L. pollen to simulated acid rain. New Phytol. 97, 63–70. https://doi.org/10.1111/j.1469-8137.1984.tb04109.x.

Dimiev, A.M., Alemany, L.B., Tour, J.M., 2013. Graphene oxide. Origin of acidity, its instability in water, and a new dynamic structural model. ACS Nano 7, 576–588. https://doi.org/10.1021/nn3047378.

Domozych, D., Fujimoto, C., LaRue, T., 2013. Polar expansion dynamics in the plant kingdom: a diverse and multifunctional kourney on the path to pollen tubes. Plants 2, 148–173. https://doi.org/10.3390/plants2010148.

Dreyer, D.R., Park, S., Bielawski, W., Ruoff, R.S., 2010. The chemistry of graphene oxide. Chem. Soc. Rev. 39, 228–240. https://doi.org/10.1039/b917103g.

Du Bay, D.T., Murdy, W.H., 1983. The impact of sulfur dioxide on plant sexual reproduction: *in vivo* and *in vitro* effects compared. J. Environ. Qual. 12, 147. https://doi.org/10.2134/jeq1983.00472425001200010027x.

DuBay, D.T., Murdy, W.H., 1983. Direct adverse effects of SO2 on seed set in *Geranium carolinianum* L.: a consequence of reduced pollen germination on the stigma. Bot. Gaz. 144, 376–381. https://doi.org/10.1086/337386.

Fadeel, B., Bussy, C., Merino, S., Vázquez, E., Flahaut, E., Mouchet, F., Evariste, L., Gauthier, L., Koivisto, A.J., Vogel, U., Martín, C., Delogu, L.G., Buerki-Thurnherr, T., Wick, P., Beloin-Saint-Pierre, D., Hischier, R., Pelin, M., Candotto Carniel, F., Tretiach, M., Cesca, F., Benfenati, F., Scaini, D., Ballerini, L., Kostarelos, K., Prato, M., Bianco, A., 2018. Safety assessment of graphene-based materials: focus on human health and the environment. ACS Nano 12, 10582–10620. https://doi.org/10.1021/acsnano.8b04758.

Ferrari, A.C., Meyer, J.C., Scardaci, V., Casiraghi, C., Lazzeri, M., Mauri, F., Piscanec, S., Jiang, D., Novoselov, K.S., Roth, S., Geim, A.K., 2006. Raman spectrum of graphene and graphene layers. Phys. Rev. Lett. 97, 1–4. https://doi.org/10.1103/PhysRevLett.97.187401.

Ge, L.L., Xie, C.T., Tian, H.Q., Russell, S.D., 2009. Distribution of calcium in the stigma and style of tobacco during pollen germination and tube elongation. Sex. Plant Reprod. 22, 87–96. https://doi.org/10.1007/s00497-009-0094-3.

Gonzáles-Domínguez, J.M., León, V., Lucío, M.I., Prato, M., Vázquez, E., 2018. Production of ready-to-use few-layer graphene in aqueous suspensions. Nat. Protoc. 13, 495–506. https://doi.org/10.1038/nprot.2017.142.

Guo, Z., Xie, C., Zhang, P., Zhang, J., Wang, G., He, X., Ma, Y., Zhao, B., Zhang, Z., 2017. Toxicity and transformation of graphene oxide and reduced graphene oxide in bacteria biofilm. Sci. Total Environ. 580, 1300–1308. https://doi.org/10.1016/j.scitotenv.2016.12.093.

Heslop-Harrison, J., Heslop-Harrison, Y., Shivanna, K.R., 1984. The evaluation of pollen quality, and a further appraisal of the fluorochromatic (FCR) test procedure. Theor. Appl. Genet. 67, 367–375. https://doi.org/10.1007/BF00272876.

Holdaway-Clarke, T.L., Hepler, P.K., 2003. Control of pollen tube growth: role of ion gradients and fluxes. New Phytol. 159, 539–563. https://doi.org/10.1046/j.1469-8137.2003.00847.x.

Jiang, J., Zhang, Z., Cao, J., 2013. Pollen wall development : the associated enzymes and metabolic pathways. Plant Biol (Stuttg). 15, 249–263. https://doi.org/10.1111/j.1438-8677.2012.00706.x.

Jiang, Y., Raliya, R., Liao, P., Biswas, P., Fortner, J.D., 2017. Graphene oxides in water: assessing stability as a function of material and natural organic matter properties. Environ. Sci. Nano 4, 1484–1493. https://doi.org/10.1039/c7en00220c.

Kabiri, S., Degryse, F., Tran, D.N.H., Da Silva, R.C., McLaughlin, M.J., Losic, D., 2017. Graphene oxide: a new carrier for slow release of plant micronutrients. ACS Appl. Mater. Interfaces 9, 43325–43335. https://doi.org/10.1021/acsami.7b07890.

Litschke, T., Kuttler, W., 2008. On the reduction of urban particle concentration by vegetation - a review. Meteorol. Zeitschrift 17, 229–240. https://doi.org/10.1127/0941-2948/2008/0284.

Liu, X.T., Mu, X.Y., Wu, X.L., Meng, L.X., Guan, W.B., Ma, Y.Q., Sun, H., Wang, C.J., Li, X.F., 2014. Toxicity of multi-walled carbon nanotubes, graphene oxide, and reduced graphene oxide to zebrafish embryos. Biomed. Environ. Sci. 27, 676–683. https://doi.org/10.3967/bes2014.103.

Liu, J., Zhao, Q., Zhang, X., 2017. Structure and slow release property of chlorpyrifos/graphene oxide-ZnAl-layered double hydroxide composite. Appl. Clay Sci. 145, 44–52. https://doi.org/10.1016/j.clay.2017.05.023.

Miraftab, R., Xiao, H., 2019. Feasibility and potential of graphene and its hybrids with cellulose as drug carriers: a commentary. J. Bioresour. Bioprod. 4, 200–201. https://doi.org/10.12162/jbb.v4i4.013.

Mogera, U., Dhanya, R., Pujar, R., Narayana, C., Kulkarni, G.U., 2015. Highly decoupled graphene mltilayers: turbostraticity at its best. J. Phys. Chem. Lett. 6, 4437–4443. https://doi.org/10.1021/acs.jpclett.5b02145.

Montagner, A., Bosi, S., Tenori, E., Bidussi, M., Alshatwi, A.A., Tretiach, M., Prato, M., Syrgiannis, Z., 2017. Ecotoxicological effects of graphene-based materials. 2d Mater. 4, 1–9. https://doi.org/10.1088/2053-1583/4/1/012001.

Novoselov, K.S., Fal'Ko, V.I., Colombo, L., Gellert, P.R., Schwab, M.G., Kim, K., 2012. A roadmap for graphene. Nature 490, 192–200. https://doi.org/10.1038/nature11458.

Pasqualini, S., Tedeschini, E., Frenguelli, G., Wopfner, N., Ferreira, F., D'Amato, G., Ederli, L., 2011. Ozone affects pollen viability and NAD(P)H oxidase release from *Ambrosia artemisiifolia* pollen. Environ. Pollut. 159, 2823–2830. https://doi.org/10.1016/j.envpol.2011.05.003.

Pelin, M., Fusco, L., Martín, C., Sosa, S., Frontiñán-Rubio, J., González-Domínguez, J.M., Durán-Prado, M., Vázquez, E., Prato, M., Tubaro, A., 2018. Graphene and graphene oxide induce ROS production in human HaCaT skin keratinocytes: the role of xanthine oxidase and NADH dehydrogenase. Nanoscale 10, 11820–11830. https://doi.org/10.1039/c8nr02933d.

Potocký, M., Jones, M.A., Bezvoda, R., Smirnoff, N., Žárský, V., 2007. Reactive oxygen species produced by NADPH oxidase are involved in pollen tube growth. New Phytol.

174, 742–751. https://doi.org/10.1111/j.1469-8137.2007.02042.x.
Qi, L., Wang, S., 2019. Sources of black carbon in the atmosphere and in snow in the Arctic. Sci. Ton. Env. 691, 442–454. https://doi.org/10.1016/j.scitotenv.2019.07.073.
Ramanathan, V., Carmichael, G., 2008. Global and regional climate changes due to black carbon. Nat. Geosci. 1, 221–227. https://doi.org/10.1038/ngeo156.
Seabra, A.B., Paula, A.J., De Lima, R., Alves, O.L., Durán, N., 2014. Nanotoxicity of graphene and graphene oxide. Chem. Res. Toxicol. 27, 159–168. https://doi.org/10.1021/tx400385x.
Song, J., Zhang, H., Duan, C., Cui, X., 2018. Exogenous application of succinic acid enhances tolerance of *Larix olgensis* seedling to lead stress. J. For. Res. 29, 1497–1505. https://doi.org/10.1007/s11676-017-0579-0.
Speranza, A., Leopold, K., Maier, M., Rita, A., Scoccianti, V., Bo, C., 2010. Pd-nanoparticles cause increased toxicity to kiwifruit pollen compared to soluble Pd(II). Environ. Pollut. 158, 873–882. https://doi.org/10.1016/j.envpol.2009.09.022.
Speranza, A., Crinelli, R., Scoccianti, V., Rita, A., Iacobucci, M., Bhattacharya, P., Chun, P., Bigea, D., Bologna, U., Irnerio, V., Biomolecolari, S., Bo, U.C., Bo, U.C., 2013. *In vitro* toxicity of silver nanoparticles to kiwifruit pollen exhibits peculiar traits beyond the cause of silver ion release. Environ. Pollut. 179, 258–267. https://doi.org/10.1016/j.envpol.2013.04.021.
Suzuki, N., Miller, G., Morales, J., Shulaev, V., Torres, M.A., Mittler, R., 2011. Respiratory burst oxidases: the engines of ROS signaling. Curr. Opin. Plant Biol. 14, 691–699. https://doi.org/10.1016/j.pbi.2011.07.014.
Tu, Y., Lv, M., Xiu, P., Huynh, T., Zhang, M., Castelli, M., Liu, Z., Huang, Q., Fan, C., Fang, H., Zhou, R., 2013. Destructive extraction of phospholipids from *Escherichia coli* membranes by graphene nanosheets. Nat. Nanotechnol. 8, 594–601. https://doi.org/10.1038/nnano.2013.125.
Wang, Q., Zhao, S., Zhao, Y., Rui, Q., Wang, D., 2014. Toxicity and translocation of graphene oxide in *Arabidopsis* plants under stress conditions. RSC Adv. 4, 60891–60901. https://doi.org/10.1039/c4ra10621k.
Wang, H.X., Maher, B.A., Ahmed, I.A.M., Davison, B., 2019a. Efficient removal of ultrafine particles from diesel exhaust by selected tree species: implications for roadside planting for improving the quality of urban air. Environ. Sci. Technol. 53, 6906–6916. https://doi.org/10.1021/acs.est.8b06629.
Wang, X., Xie, H., Wang, Z., He, K., 2019b. Graphene oxide as a pesticide delivery vector for enhancing acaricidal activity against spider mites. Colloids Surf. B Biointerfaces 173, 632–638. https://doi.org/10.1016/j.colsurfb.2018.10.010.
Wolters, J.H.B., Martens, M.J.M., 1987. Effects of air pollutants on pollen. Bot. Rev. 53, 372–414.
Zeng, W., Wu, S., Pang, L., Sun, Y., Chen, Z., 2017. The utilization of graphene oxide in traditional construction materials: asphalt. Materials 10. https://doi.org/10.3390/ma10010048.
Zhang, W., Wang, C., Li, Z., Lu, Z., Li, Y., Yin, J.J., Zhou, Y.T., Gao, X., Fang, Y., Nie, G., Zhao, Y., 2012. Unraveling stress-induced toxicity properties of graphene oxide and the underlying mechanism. Adv. Mater. 24, 5391–5397. https://doi.org/10.1002/adma.201202678.
Zhang, M., Gao, B., Chen, J., Li, Y., Creamer, A.E., Chen, H., 2014. Slow-release fertilizer encapsulated by graphene oxide films. Chem. Eng. J. 255, 107–113. https://doi.org/10.1016/j.cej.2014.06.023.
Zhao, J., Cao, X., Wang, Z., Dai, Y., Xing, B., 2017. Mechanistic understanding toward the toxicity of graphene-family materials to freshwater algae. Water Res. 111, 18–27. https://doi.org/10.1016/j.watres.2016.12.037.
Zienkiewicz, K., Rejón, J.D., Suárez, C., Castro, A.J., de Dios Alché, J., Rodríguez García, M.I., 2011. Whole-organ analysis of calcium behaviour in the developing pistil of olive (*Olea europaea* L.) as a tool for the determination of key events in sexual plant reproduction. BMC Plant Biol. 11. https://doi.org/10.1186/1471-2229-11-150.